Analysis of Field-Measured Reversible Deformations in Masonry Cavity Walls

A. J. Lohonyai[1], Y. Korany[2], and N. Trovato[3]

INTRODUCTION

Distress and failure of clay brick masonry facades is often believed to be the result of high compressive stresses arising from excessive vertical differential movement between the clay brick masonry facade and structural backing wall. Vertical movements are caused by a combination of elastic deformation of the load-bearing members, creep, shrinkage, or swelling due to drying or wetting, freezing expansion, and thermal expansion or contraction (Peraza (2009), IRCI (2008), Straube and Burnett (2005)). Guidelines currently used by designers to estimate the unrestrained vertical deformations of masonry are based on laboratory observations of individual units (MSJC (2011), NRC (2010), ASTM (2010), BIA (2006), CEN (2005), NCMA (2005), CSA (2004)). However, research has shown that the effects of the mortar joints on the overall deformation of masonry walls are significant (Jessop (1980)). The presence of mortar joints should not be ignored when analyzing a masonry assemblage, particularly where the behavior of the units is dissimilar to the behavior of the mortar. Furthermore, long-term deformations in masonry are not a simple linear addition of elastic, moisture, and creep components, as there are potentially significant interactions between moisture, stiffness, strength, and creep (Sayed-Ahmed et al (1998), Forth et al (2000), Amde et al (2007)). Accordingly, design guidelines may not yield consistently reasonable estimates of axial deformations in masonry walls.

The problem of differential movement in masonry walls has been discussed in the literature for decades (Plewes (1970), Peraza (2009)), but to the knowledge of the authors, has rarely been measured in modern buildings in service. Intensive research efforts through the 1970s and 1980s discussed several potential sources of deformation and attempted to quantify their effects analytically (Plewes, (1970) (1976) (1977), Grimm (1975) (1982), Suter and Hall (1976), Grimm and Fowler (1979), Anand and Gandhi (1983), Fenton and Suter (1985a) (1985b), Yura (1986), Brooks (1987a) (1987b)). The various analytical studies were in agreement that restrained deformations in masonry led to high compressive stresses in masonry facades, supporting conclusions that restrained movement was causing cracking, spalling, bulging, and buckling failures. More recent laboratory experimental work was carried out to collect new data on the elastic, shrinkage, and creep characteristics of masonry (Davison (1980), Shrive and England (1981), Brooks and Abdullah (1990), Drysdale and Khattab (1995), Sayed-Ahmed et al (1998)). Guidelines for movement joint design were developed and revised based on the results of these laboratory investigations with the goal of obviating distress and failure in masonry facades.

While the laboratory experimental work on masonry units and small assemblages has proven valuable in enhancing understanding of masonry deformation, there is clearly a need for data on the behavior of masonry walls in real buildings. Movement joint design guidelines do not agree well with one another (NRC (2010), ASTM (2010), CSA (2004)), and despite all the information now available to designers, masonry facade failures continue to occur at an alarming rate (Grimm (2000), Kvande and Lisø (2009)). There is a significant scarcity of data on long-term deformations and differential movements in masonry walls measured in buildings of modern construction under field conditions. Hughes and Harvey (1995) measured axial strains in a heavily loaded wall in a masonry tower over a period of 6000 days and found that creep predictions based on comparatively short-term laboratory studies underestimated the long-term strains measured in the field. Kuzik et al. (1999) monitored differential movement in masonry cavity walls over a period of 1322 days beginning from the building's construction. Kuzik et al. commented that a lot of emphasis is placed on excessive expansion of the clay brick wythe in masonry facade failure analyses, but their results indicated that the permanent volume of the clay brick wythe was relatively stable and almost all of the differential movement observed was attributable to the shrinkage of the concrete block wythe. They offered the explanation that shrinkage and creep in the mortar joints counteracted the permanent moisture expansion of the clay bricks. Kuzik et al. only commented on the impact of permanent moisture-related deformation on differential movement, though design guidelines indicate that thermal strains and reversible moisture strains combined are as much as 1 to 4 times the permanent moisture strain (MSJC (2011), NRC (2010), BIA (2006), CEN (2005), NCMA (2005), CSA (2004)).

1. Forensic engineer, Sintra Engineering Inc., Edmonton, AB, Canada, alohonyai@sintraeng.com
2. TMS Member, Associate Professor, Dept. of Civil & Environmental Engineering, University of Alberta, Edmonton, AB, Canada, ykorany@ualberta.ca
3. Managing Principal, Building Science and Restoration, Read Jones Christoffersen, Edmonton, AB, Canada, ntrovato@rjc.ca

The main objective of this investigation was to analyze the data record created by a remote monitoring system installed by the authors in a 17-year-old clock tower in St. Albert, Alberta, shown in a section in Figure 1, in the autumn of 2012 (Lohonyai et al (2014)). Measurements of vertical deformation, temperature, and humidity were collected hourly for a period 638 days, capturing the effects of daily and seasonal climatic variations on the differential movement in the masonry cavity walls. The St. Albert clock tower and the remote monitoring system are described briefly below. Further details have been reported elsewhere (Lohonyai et al (2014)).

ST. ALBERT CLOCK TOWER

The St. Albert clock tower, shown in Figure 1, was erected in 1995 in St. Albert, Alberta, Canada to serve both as a public landmark for the city and as a research structure for the University of Alberta. The instrumented cavity walls are each about 7'-10" (2.4 m) wide by 39'-4" (12 m) tall, designed and detailed to resist only self-weight and out-of-plane wind pressure. Gravity loads are resisted by L-shaped columns located at the tower's four corners. Movement joints isolate the walls from the main structural component, allowing the walls to expand or contract horizontally and vertically freely.

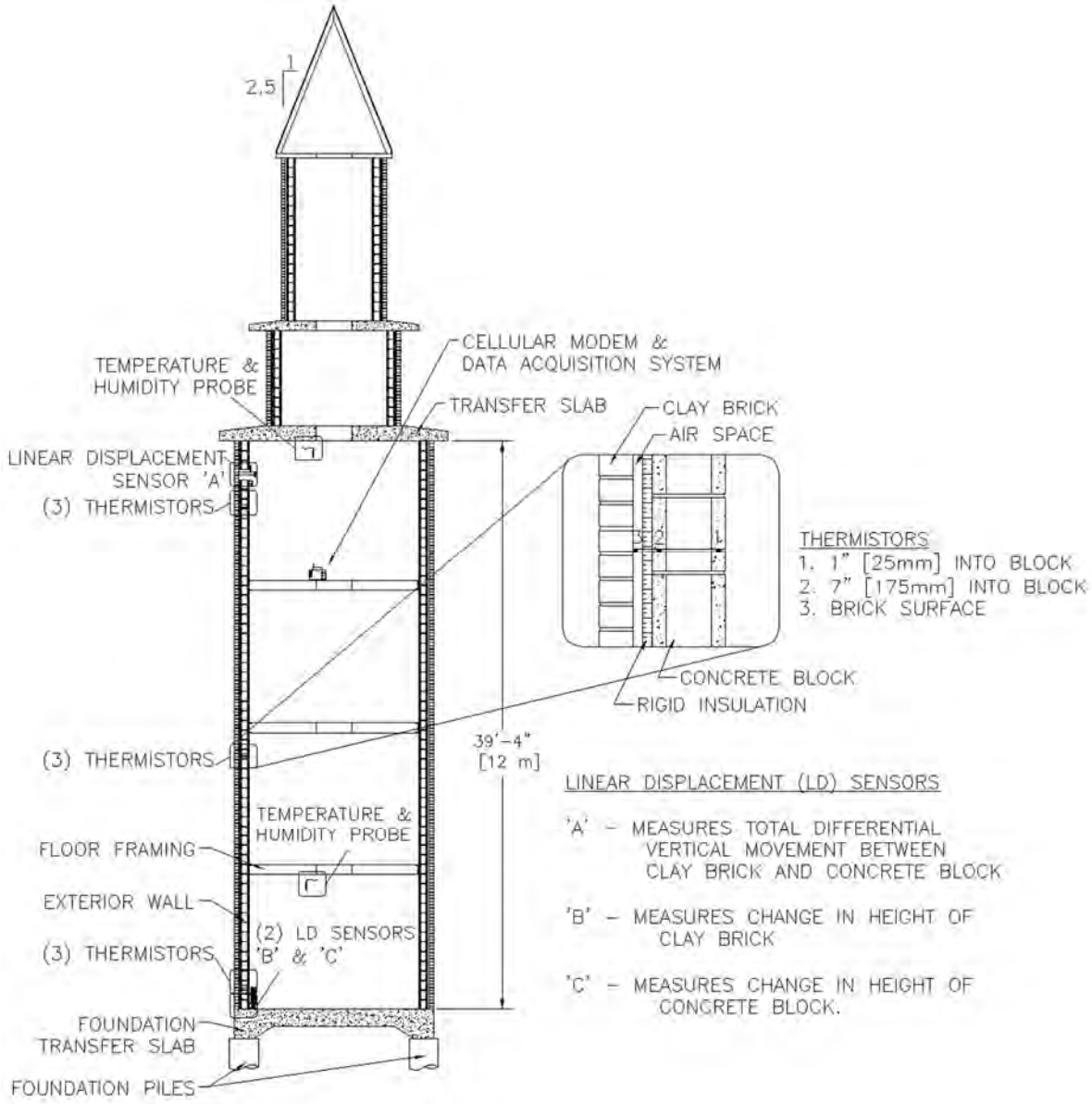

Figure 1 - Section View Through the Instrumented St. Albert Clock Tower

The walls each vary slightly in construction because the building was originally designed with the intent of researching the effects of variations in construction details on deformations. The basic construction of the wall consists of nominal 8” (200 mm) concrete block inner wythe, rigid insulation and air space, and nominal 4” (100 mm) clay brick outer wythe. Table 1 summarizes the variations in cavity width, insulation thickness, and type of masonry tie between the four walls. The shear transfer ties used in the east, south, and west walls are Block Shear™ connectors (FERO Corporation (2014)).

The clock tower is located about 2170’ (660 m) above sea level at 53°37’56”N latitude and 113°37’24”W longitude. St. Albert is in a very cold climate, typically experiencing about 9360 65 °F heating degree days (5200 18 °C heating degree days) annually, with mean annual temperature and precipitation of about 39 °F (3.9 °C) and 19” (480 mm), respectively.

REMOTE MONITORING SYSTEM

The remote monitoring system consists of a multipurpose measurement and control data logger, a wireless cellular modem, two 16/32 channel multiplexers, 12 linear displacement sensors, 36 thermistors, two resistance temperature detectors, and two capacitive humidity sensors. The data logger was programmed to engage the multiplexers and cycle through each sensor, reading and recording the output of all 52 installed sensors in rapid succession once per hour. Raw data can be collected by connecting to the data logger remotely over the internet, thus eliminating the need for attending the site.

Eight spring-loaded linear displacement sensors (LD sensors) were installed to measure axial deformations: one sensor per wythe per wall (‘B’ and ‘C’ in Figure 1 and Figure 2). As shown in Figure 2, a hollow steel square section with suspended solid steel weight was anchored to each wythe at approximately 36’ (11 m) elevation (location ‘A’ in Figure 1). The LD sensors were mounted under the suspended steel weights to measure their change in vertical position. Figure 2 shows the LD sensors under the steel weights before installing the protective sleeves that ensured the weights remained aligned over the sensors. Changes in the readings of the LD sensors, corrected for thermoelastic and creep effects in the measuring setup, correspond to changes in the length of the respective wythes. Another four LD sensors were mounted to the steel tubes on the concrete wythes with the probe tips in contact with the steel tubes attached to the clay brick wythes, thereby measuring vertical differential movement in each cavity wall directly. Figure 2 shows the sensor arrangement to measure the differential movement directly.

Table 1. Construction Details of the St. Albert Clock Tower Cavity Walls

Wall Orientation	Air Space Thickness	Insulation Thickness	Type of Ties
North Wall	1” (25 mm)	1” (25 mm)	Vertically slotted
East Wall	1” (25 mm)	no cavity insulation	Shear transfer
South Wall	1” (25 mm)	2” (50 mm)	Shear transfer
West Wall	2” (50 mm)	2” (50 mm)	Shear transfer

Figure 2 - Sensor 'A' (left) and Sensors 'B' and 'C' (right)

DEFORMATIONS IN MASONRY WALLS

Deformations in masonry can be categorized as permanent or reversible. Permanent deformations include drying shrinkage of mortar and concrete masonry units, moisture-induced swelling of fired clay bricks, and creep under long-term stresses. Reversible deformations include expansion or contraction following an increase or decrease in temperature and/or moisture content, and freezing or thawing of trapped pore water. Elastic shortening or lengthening arising from the short-term application or removal of axial compressive stresses are also considered reversible deformations. The exterior masonry walls of the St. Albert clock tower are not load-bearing and were a little more than 17 years old at the time this investigation began. Therefore, it is assumed that all permanent deformations have already taken place and that elastic strains are negligible.

Masonry thermal strain, ε_t, is typically calculated using Equation (1), where α is the linear coefficient of thermal expansion of the masonry and ΔT is the change in the masonry's temperature. Recommended values for α given in various design guidelines are summarized in Table 2. For clay brick and hollow concrete block, α is commonly given to be about 4×10^{-6} in/in/°F (7×10^{-6} mm/mm/°C) and 5×10^{-6} in/in/°F (9×10^{-6} mm/mm/°C), respectively.

$$\varepsilon_t = \alpha \Delta T \tag{1}$$

In the design of movement joints, it is important to appropriately define the design temperature range. The temperature of a building facade can be much warmer than the outdoor air temperature on bright sunny days. For walls built of heavy materials like concrete and masonry, the 2010 National Building Code of Canada Commentaries (NBCC Commentaries) recommends that the peak design temperature of the facade be taken to be 18-27 °F (10-15 °C) higher than the design outdoor air temperature (NRC (2010)). The design outdoor air temperature prescribed in the 2010 NBCC Commentaries is the 97.5 percentile July dry bulb temperature, which is 82 °F (28 °C) for the location of the St. Albert clock tower. ASTM C1472-10 (ASTM (2010)) takes a slightly more rational approach in the form of Equation (2), estimating peak surface temperature, $T_{s,max}$, from the design air temperature, T_a, solar absorption coefficient, A, and empirical heat capacity constant, H. The product of A and H is added to the design air temperature and represents the maximum expected overheating due to solar radiation, accounting for the influence of different thermal mass and solar reflectance of different materials. ASTM C1472-10 recommends H = 75 °F (42 °C) for materials with high heat capacity like masonry, provided that the building is not surrounded by highly reflective surfaces nearby. The clay bricks used in the facade of the St. Albert clock tower are an earthy red color. ASTM C1472-10 recommends a range for A of 0.65 to 0.85 for that color. Therefore, ASTM C1472-10 suggests that solar radiation can raise the temperature of the clay brick facade to 49 to 64 °F (27 to 36 °C) above the outdoor air temperature at the St. Albert clock tower. ASTM C1472-10 differs slightly from the 2010 NBCC Commentaries by defining the design air temperature to be the 99.6 percentile annual dry bulb temperature. The two definitions are nearly equivalent; for the St. Albert clock tower, the ASTM C1472-10 design air temperature is still 82 °F (28 °C).

$$T_{s,max} = T_a + A \cdot H \tag{2}$$

Reversible moisture strains, $\varepsilon_{m,r}$, arise from variations in a material's moisture content, which is influenced by humidity, temperature, and rain. Design guidelines recommend limiting design values for reversible moisture strain rather than prescribing some predictive function of one or more variables. Recommended values of $\varepsilon_{m,r}$ given in various design guidelines are summarized in Table 2. The values of $\varepsilon_{m,r}$ in the Canadian standard CSA S304.1-04 agree with those in ASTM C1472-10, but are up to twice the values recommended by the 2010 NBCC Commentaries. Several other masonry guidelines (BIA (2006), NCMA (2005), MSJC (2011), CEN (2005)) do not address reversible moisture strain explicitly, either ignoring it or accounting for it in the recommended permanent moisture strain.

Table 2. Reversible Deformation Parameters of Masonry Reported in Various Design Guidelines

Parameter	Units	Clay Brick Masonry	Normal Weight Concrete Block Masonry	Source
α	in/in/°F	3.9 to 5.0×10^{-6} 3.9×10^{-6} 4.0×10^{-6} – 4.0×10^{-6} 2.2 to 4.4×10^{-6} 2.5×10^{-6}	4.4 to 5.6×10^{-6} 5.6×10^{-6} 4.5×10^{-6} 2.5 to 5.5×10^{-6} 4.5×10^{-6} 3.3 to 6.7×10^{-6} 5.2×10^{-6}	CSA 2004 NRC 2010 BIA 2006 NCMA 2005 MSJC 2011 CEN 2005 ASTM 2010
$\varepsilon_{m,r}$	in/in	$\pm200\times10^{-6}$ $\pm100\times10^{-6}$ $\pm200\times10^{-6}$	±200 to $\pm400\times10^{-6}$ $\pm200\times10^{-6}$ ±200 to $\pm400\times10^{-6}$	CSA 2004 NRC 2010 ASTM 2010

Freezing expansion is not addressed in most design guidelines and is usually ignored in practice (BIA (2006)), though some experimental research has indicated that freezing expansion can be on the order of 0.1% (Davison (1980)). Where clay brick is expected to be saturated or nearly saturated and exposed to temperatures below 14 °F (-10 °C), BIA (2006) recommends 0.02% expansion to account for freezing of trapped pore water.

Design guidelines suggest that total deformations in masonry be considered as the worst case of the linear combination of permanent and reversible strains. In addition to assuming that the permanent strains at the St. Albert clock tower have already occurred and that the elastic strains are negligible, freezing expansion was also ignored. While St. Albert does experience the requisite low temperatures, in the authors' opinion it is unlikely for the clay brick wythe to be sufficiently saturated at the time of freezing for appreciable expansion to occur. Therefore, the deformations observed in this investigation are considered to be only the combination of thermal and reversible moisture strains, expressed by Equation (3). Using thermal expansion coefficients and reversible moisture-induced strain values provided in design guidelines like CSA S304.1-04 and the 2010 NBCC Commentaries, a range of possible total reversible strains, ε_{tot}, in the masonry of the clock tower can be predicted from Equation (3). Equation (4) represents the differential strain, equal to the difference between the strain in the clay brick wythe, ε_{br}, and the strain in the concrete block wythe, ε_{bl}, each of which are calculated from Equation (3). The datum used in this investigation was established by taking the average of the readings from 22:00 to 03:00 on September 30th to October 1st, 2012. Averaging reduces the level of uncertainty in the datum, though the choice of datum is somewhat arbitrary since there was no way to determine the amount of differential movement present at the time the remote monitoring system was installed. The datum air conditions were 67.6 °F (19.8 °C) with 37.3% humidity inside the tower and 43.9 °F (6.6 °C) with 72.7% humidity outside the tower.

$$\varepsilon_{tot} = \alpha \Delta T + \varepsilon_{m,r} \quad (3)$$

$$\Delta\varepsilon = \varepsilon_{br} - \varepsilon_{bl} \quad (4)$$

UNCERTAINTY AND POTENTIAL ERROR IN THE DATA

Though the remote monitoring system was designed to maximize accuracy, some degree of uncertainty in the observed deformations is recognized. Economic and accurate measurement of movements on the order of hundredths to thousandths of an inch over a gauge length of a little more than 36' (11 m) for several months and in widely varying temperatures is challenging. However, the authors are confident that at least the measured movements larger than about 0.040" (1.0 mm) are meaningful and reasonably accurate. A detailed error analysis was conducted and the 95% confidence limits were estimated accordingly. Sources of error investigated were: nonlinearity and hysteresis effects in the LD sensors, temperature effects on the LD sensors, uncertainty in the calibration data provided by the manufacturer of the LD sensors, reading and resolution error introduced by the data logger, deformations caused by wind loads, deformations caused by thermal gradients through the wall, and uncertainty in the creep correction model parameters used to correct for long-term creep in the setup. Table 3 provides a summary of the sources of error and the amount of uncertainty they contribute to the individual wythe and differential movement measurements. The sources of error identified are largely independent of each other and therefore the errors from each source were taken to be independent and additive.

Table 3. Potential Sources of Error and Their Contribution to Uncertainty in the Measurements

Potential Source of Error	Limit Error on Individual Wythe Movement	Limit Error on Differential Movement
Nonlinearity and hysteresis effects on LD sensors	± 0.0020" (0.05 mm)	± 0.0016" (0.04 mm)
Temperature effects on LD sensors	± 0.0012" (0.03 mm)	± 0.0031" (0.08 mm)
Uncertainty in LD sensor calibration	± 0.0035" (0.09 mm)	± 0.0031" (0.08 mm)
Reading and resolution error	± 0.0012" (0.03 mm)	± 0.0012" (0.03 mm)
Wind-induced deflections	< ± 0.0004" (0.01 mm)	< ± 0.0004" (0.01 mm)
Thermal gradient induced deflections	± 0.0051" (0.13 mm)	± 0.0024" (0.06 mm)
Uncertainty in creep model	± 0.0105" (0.27 mm)	≈ 0
Sum of errors*	± 0.023" (0.58 mm)	± 0.011" (0.28 mm)

*Maximum errors from each source do not all occur simultaneously in the same sensor. Due to this fact, the maximum sum of errors presented in the table is not exactly equal to the sum of the maximum individual source errors above.

The LD sensor outputs voltage that is approximately a linear function of the displacement of the probe tip. Non-linearity errors refer to the deviation between the assumed linear voltage-displacement relation and the true displacement. The sensor also experiences some hysteresis, meaning at a given true displacement, the reading will be slightly different if the tip moved down to the point than if it moved up to that point. The magnitude of non-linearity and hysteresis error is unique to each sensor and was provided by the manufacturer. The combined effects of non-linearity and hysteresis introduce limit errors of up to ± 0.0016" (0.04 mm) to the measured differential movement and ± 0.0020" (0.05 mm) to the individual wythe measurements.

Temperature also has some effect on the sensor, up to 0.0056% of the full stroke per degree Fahrenheit (0.01% of the full stroke per degree Celsius) temperature change within the operating range of 14 to 158 °F (-10 to +70 °C). The temperature effect is a function of the temperature inside the tower at the time of the reading. Based on the wide range of recorded temperatures, thermal effects on the LD sensor introduce as much as ± 0.0031" (0.08 mm) of uncertainty in the differential movement and ± 0.0012" (0.03 mm) in the individual wythe movement. The range of uncertainty due to temperature is much smaller for the individual wythe movement because temperatures of those sensors are much more stable. The combination of the stack effect, thermal mass of the ground, and the two space heaters to keep tower maintenance personnel more comfortable in the winter keep the sensors measuring the individual wythes cooler in the summer and warmer in the winter.

The voltage-displacement relation assumes that the calibration data is accurate. However, assuming that the limit errors in the manufacturer-reported data are equal to ± 0.5 units of the smallest reported digit, then some uncertainty will be introduced that is a function of the measurement itself. Uncertainty in the sensor calibration data introduces as much as ± 0.0031" (0.08 mm) and ± 0.0035" (0.09 mm) of error in the differential movement and individual wythe displacement, respectively.

Reading and resolution errors are introduced by the data logger because the logger excites the sensor with an input voltage that can only be produced within a certain tolerance. The logger also has a certain error tolerance in reading voltages, so additional uncertainty is introduced in reading the voltage output from the sensor. Combined, these potential errors amount to up to ± 0.0012" (0.03 mm) in both the measured differential movement and the individual wythe displacement.

Wind was considered as a possible source of error, causing curvatures and lateral deflections in the walls and overall structure that would influence the sensor readings. However, the clock tower is a relatively stiff structure and most of the time wind velocities are low, inducing rather small forces and deflections. The 95 percentile hourly averaged wind velocity at the St. Albert clock tower was calculated to be 18 mph (8.1 m/s). Equivalent wind pressures were doubled to account for gusting, but deflections output from the elastic frame analysis model of the tower were still quite small. Wind effects were estimated to contribute less than ± 0.0004" (0.01 mm) of error 95% of the time.

A temperature difference through the thickness of a wall will cause a tendency for the wall to curve. Using an elastic frame analysis model, the effect of temperature gradient through the clay brick wythe and concrete block wythe was quantified. Temperature gradient in the concrete block wythe can be determined from the data collected, so the data processing algorithm includes a correction for thermal gradients in the concrete block wythe. However, the gradient in the clay brick wythe was not calculable from the collected data because only the inner surface temperature was measured. An estimate of the worst case thermal gradient in the clay brick wythe was obtained using the results of a thermal analysis of the clock tower using WUFI Plus, a program for performing whole building energy simulation and hygrothermal analysis of building envelopes (FIBP (2011)). Based on these estimated gradients, the limit error in the differential movement and individual wythe movement is estimated to be up to ± 0.0024" (0.06 mm) and ± 0.0051" (0.13 mm), respectively.

The system experiences some low-temperature creep under the long-term tensile stresses applied by the suspended weights. Only the individual wythe measurements are affected. A simple expression was developed to correct for creep effects (Lohonyai et al (2014)). While the model appears to accurately estimate creep strains, uncertainty in these corrections would introduce errors that grow with time. In the 638-day record analyzed in this study, the error could be as much as ± 0.0105" (0.27 mm) on individual wythe measurements. It should be noted that errors in the creep model would be systematic rather than randomly distributed, so measurements in all four walls and both clay brick and block wythes would be affected equally. Thus, the effect of uncertainty in the creep model on vertical differential movement is negligible.

Summing up all identified sources of error, the differential movements are estimated to be consistently accurate within ± 0.011" (0.28 mm). The individual wythe measurements are estimated to be consistently accurate within ± 0.023" (0.58 mm).

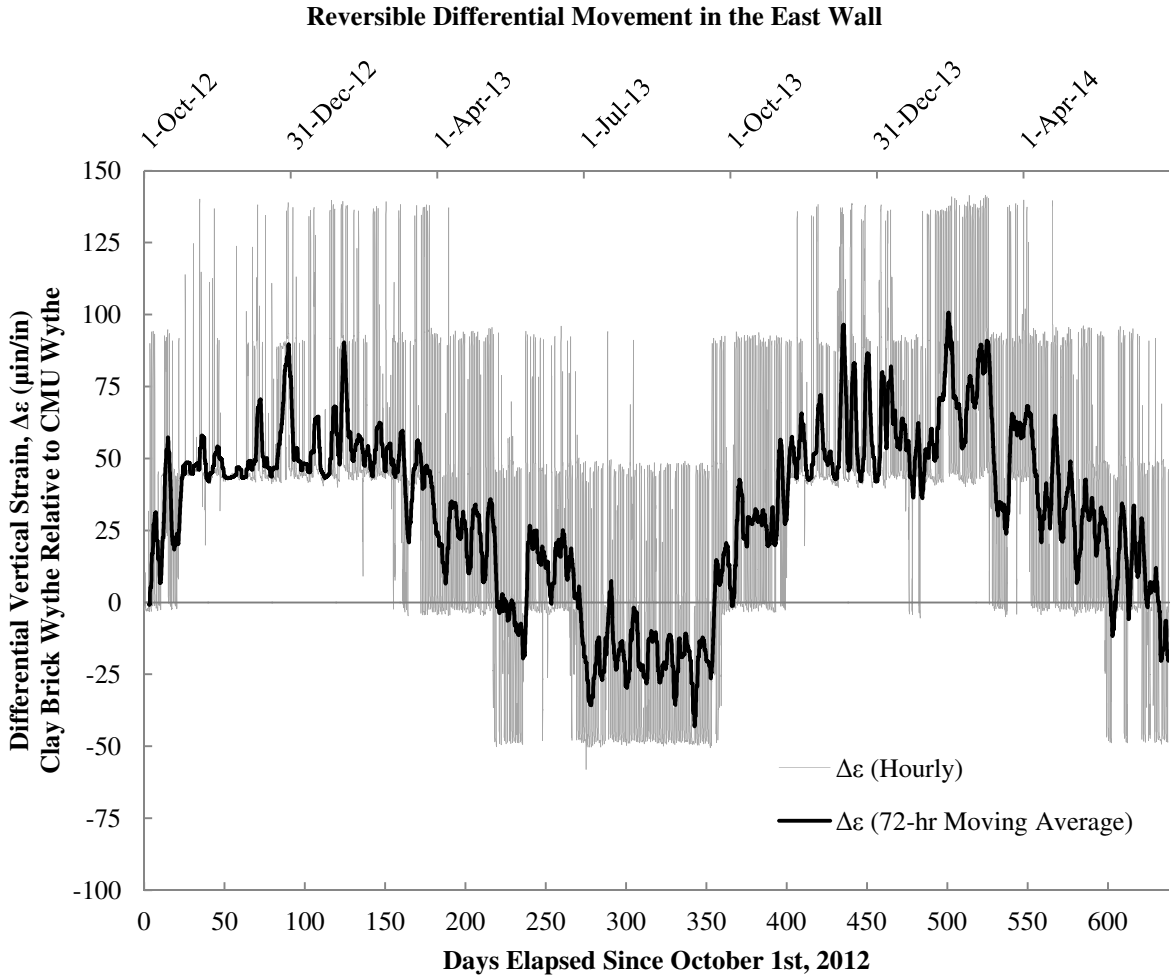

Figure 3 - Reversible Differential Movement Measured in the East Wall Over Time

OBSERVATIONS AND DISCUSSION

Observations discussed below are based on data collected between October 1st, 2012 and June 30th, 2014, a period of 638 days. Figure 3 is a plot of the hourly measured differential movement in the east wall during that time. Note that all differential movements are expressed as movement of the clay brick wythe relative to the concrete block wythe. It is readily observed that appreciable changes in the differential movement occur on a daily basis. These are attributed to solar radiation effects, which will be discussed further. Also included in Figure 3 is the 72-hour moving average differential movement, which better illustrates the seasonal trend. The general seasonal trend of the differential movement was to increase in winter (i.e. clay brick wythe appears to lengthen relative to the concrete block wythe) and decrease in summer (i.e. clay brick wythe appears to shorten relative to the concrete block wythe). This behavior is explained by a higher coefficient of thermal expansion in the concrete block wythe and the fact that the building is unconditioned. With no heating or cooling system, both wythes cool in winter and heat up in summer. While variations in the temperature of the clay brick wythe are much greater than in the concrete block wythe, the seasonal trend in temperature is consistent in both wythes. The concrete block wythe experiences greater thermal movements than the clay brick wythe for the same temperature difference. So in the winter season, though both wythes have shortened, the concrete block wythe shortens by a larger amount than the clay brick wythe. It must also be emphasized that both mortar and clay bricks comprise the outer wythe of the tower. This composite assembly of materials with dissimilar deformation characteristics will not behave as individual clay bricks behave in laboratory experiments.

Table 4. Extreme Vertical Differential Movement of the Facade Relative to the Backing Wall

Wall	Extreme Positive Movement	Date and Time	Extreme Negative Movement	Date and Time
North	0.094" ± 0.008" (2.4 ± 0.2 mm)	19:00, 08-Mar-2014	0.024" ± 0.004" (0.6 ± 0.1 mm)	11:00, 18-Sep-2013
East	0.063" ± 0.012" (1.6 ± 0.3 mm)	16:00, 08-Mar-2014	0.028" ± 0.008" (0.7 ± 0.2 mm)	01:00, 03-Jul-2013
South	0.102" ± 0.008" (2.6 ± 0.2 mm)	17:00, 18-Feb-2014	0.047" ± 0.008" (1.2 ± 0.2 mm)	07:00, 03-Jul-2013
West	0.080" ± 0.008" (2.0 ± 0.2 mm)	19:00, 29-Apr-2014	0.059" ± 0.008" (1.5 ± 0.2 mm)	06:00, 03-Jul-2013

As shown in Table 4, the most extreme, directly measured differential movement observed was a 0.102" ± 0.008" (2.6 ± 0.2 mm) lengthening of the clay brick wythe relative to the concrete block wythe in the south wall at 17:00 on February 18, 2014. Dividing by the gauge length gives the peak reversible differential strain to be 230 ± 20 μin/in. At the opposite extreme, the peak differential movement observed was a 0.059" ± 0.008" (1.5 ± 0.2 mm) shortening of the clay brick wythe relative to the concrete block wythe in the west wall at 06:00 on July 3, 2013. This corresponds to a differential strain of -130 ± 20 μin/in. At first glance it looks odd that the clay brick had gotten so much shorter relative to the backing wall in July, but the temperature measurements showed that at the time the clay brick facade was near its datum temperature, while the backing wall was simultaneously more than 18 °F (10 °C) warmer than its datum temperature. The west wall's facade's minimum daily temperature routinely occurred at 06:00 or 07:00 because the clay brick cools all through the night. Therefore, the datum temperature includes some solar heating effect. The facade may have also been drying out due to the strong winds that had occurred the previous day and lack of rain for the previous five days (Environment Canada (2014)). In Table 5, design ranges of differential movement caused by reversible deformation have been presented along with the observed peak differential movement. The design values were calculated using Equations (3) and (4) and the design values α and $\varepsilon_{m,r}$ given in S304.1-04, 2010 NBCC Commentaries, and ASTM C1472-10. The table shows that the maximum differential movement observed in this investigation is greatly exceeded by the predictions of all three design guidelines, though 2010 NBCC Commentaries is clearly more lenient than S304.1-04 and ASTM C1472-10.

It appears that the maximum differential movement observed at 17:00 on February 18, 2014 can be predicted based on thermal deformations alone. At that time, the clay brick wythe had experienced significant solar irradiation and was 24.3 °F (13.5 °C) warmer than the datum temperature while the concrete block wythe was simultaneously 26.5 °F (14.7 °C) cooler than the datum temperature. Based on the range of coefficients of thermal expansion given in S304.1-04, the thermal differential movement could be in the range of 212 to 269 μin/in. Similarly, ASTM C1472-10 predicts that the thermal differential movement would be 199 μin/in. Table 6 shows the thermal differential movements predicted by other design guidelines, and all appear to agree well with the observed maximum differential movement.

However, the relative contribution of each wythe to the total differential movement suggests that other sources of movement were present. Of the 230 μin/in differential movement observed, expansion of the clay brick wythe contributed 17 to 39%. There is a large range of uncertainty in the relative contribution of the clay brick wythe because of the appreciable limit error on the individual wythe measurements. Table 6 shows that S304.1-04 predicts that 39% to 51% of the thermal differential movement would have been contributed by the clay brick wythe. The table shows that MSJC 2011 and Eurocode 6 (CEN (2005)) also predict a contribution from the clay brick wythe that is larger than observed. Evidently the clay brick wythe's total expansion was smaller than that predicted by thermal expansion alone. This might be attributed to drying shrinkage. At the time, the outdoor air was quite dry with only 34% relative humidity. The mortar and clay bricks may have been drying out and shrinking because of the combination of low ambient humidity and high solar-induced temperature. Similarly, the indoor air had only 33% relative humidity at the time, so the concrete block may also have been experiencing some reversible shrinkage. Reversible moisture movement was estimated to have caused up to about 20% of the observed 230 μin/in differential movement.

The ratio of peak reversible strain to the maximum permanent moisture strain was also considered. Kuzik et al. (1999) reported a maximum differential movement, excluding thermal movement, of approximately 0.213" (5.4 mm), i.e. 470 μin/in, 1322 days after construction. While creep likely contributed to the total deformation, most of this permanent movement was attributed to drying shrinkage because the walls bear only their own weight. Therefore, the observed maximum reversible differential movement, 230 μin/in, was approximately half (49%) of the differential movement attributed to permanent moisture changes by Kuzik et al. Peak reversible differential movement predicted by S304.1-04 is about 97% of the maximum differential movement due to permanent moisture changes. The same ratio was calculated to be 90% using the 2010 NBCC Commentaries or 68% using ASTM C1472-10.

One of the goals of the project was to determine if reversible movements could be predicted with reasonable accuracy using a simple model. A regression analysis was performed and the reversible differential movement was found to correlate remarkably well with temperature changes alone. The results of the regression analysis are given in Table 7. The coefficient of determination varied from 0.78 for the east wall to 0.83 for the north wall. The regression coefficients correspond to the coefficient of thermal expansion combined with temperature correlated moisture effects. Prevailing winds in the area are out of the west or northwest, so the north and west walls are more severely exposed to driving rain than the east and south walls. When the clay brick wythe is experiencing high temperatures, it is simultaneously drying out and experiencing some moisture-related shrinkage. The effect would typically be greater in the north and west walls because they would have more moisture to give up, having absorbed more moisture during the previous driving rain event. This might partially explain why the north and west walls have smaller regression coefficients for the clay brick temperature variable.

Another goal of the investigation was to assess whether the current design guidelines are appropriately conservative with respect to both reversible moisture strain and peak design temperature. Figure 4 shows the reversible differential vertical movement, expressed in micro inches of movement per inch of gauge length, plotted against the difference between the change in temperature of the clay brick wythe and the change in temperature of the concrete block wythe. Using Equations (3) and (4), design limits on the differential strain were calculated for the 2010 NBCC Commentaries, CSA S304.1-04, and ASTM C1472-10. The exact value of the design limit depends on both the temperature change in the clay brick, ΔT_{br}, and the temperature change in the block, ΔT_{bl}. However, it was found that the design limits could be approximated as linear functions of the difference ($\Delta T_{br} - \Delta T_{bl}$) with standard limit error of ±62 μin/in within the range of temperatures measured during this study. It can be seen in Figure 4 that the general trend in the data agrees well with the slope of the ASTM limits. This is because the coefficient of thermal expansion given for fired clay brick in ASTM C1472-10 agrees well with the observations. Both CSA S304.1-04 and the 2010 NBCC Commentaries appear to overestimate the true coefficient of thermal expansion of the clay brick wythe. Therefore, the trend in the data does not agree with the trend in the design limits calculated using CSA S304.1-04 or the 2010 NBCC Commentaries. It is also evident from Figure 4 that the design limits of the 2010 NBCC Commentaries are significantly less conservative than either CSA S304.1-04 or ASTM C1472-10, although all of the observations fall within the design limits from the three referenced documents. Some of the data points approach to within approximately 100 μin/in of the 2010 NBCC Commentaries design limits. It is possible that the limits of the 2010 NBCC Commentaries are too lenient, though this cannot be concluded from the present study alone.

Table 5. Comparison of Observed Maximum Reversible Differential Movement with Predictions Based on Design Guidelines

Source	Maximum Reversible Differential Movement (μin/in)	Contribution from Clay Brick Wythe
Observed	230 ± 20	17 to 39%
S304.1-04	869	37%
NBCC 2010	542	36%
ASTM C1472-10	826	32%

Table 6. Differential Thermal Movement Predicted by Various Design Guidelines for the Temperature Conditions Observed at 17:00 February 18, 2014

Source	Differential Thermal Movement (μin/in)	Contribution from Clay Brick Wythe
CSA S304.1-04	212 to 269	39 to 51%
2010 NBCC Commentaries	242	39%
ASTM C1472-10	199	31%
MSJC 2011	217	45%
EuroCode 6	142 to 285	23 to 55%

Table 7. Summary of the Regression Analysis for Vertical Differential Movement in the Masonry Cavity Walls

Wall	Regression Equation	Standard Error	Coefficient of Determination, R^2
North	$2.2\Delta T_{br} - 5.0\Delta T_{bL} + 36$ μin/in	± 19 μin/in	0.83
East	$3.3\Delta T_{br} - 5.7\Delta T_{bL} - 15$ μin/in	± 20 μin/in	0.78
South	$3.1\Delta T_{br} - 5.9\Delta T_{bL} + 10$ μin/in	± 24 μin/in	0.81
West	$2.6\Delta T_{br} - 5.2\Delta T_{bL} - 11$ μin/in	± 20 μin/in	0.79

ΔT_{br} = change in temperature of the clay brick facade

ΔT_{bL} = change in temperature of the concrete masonry backing wall

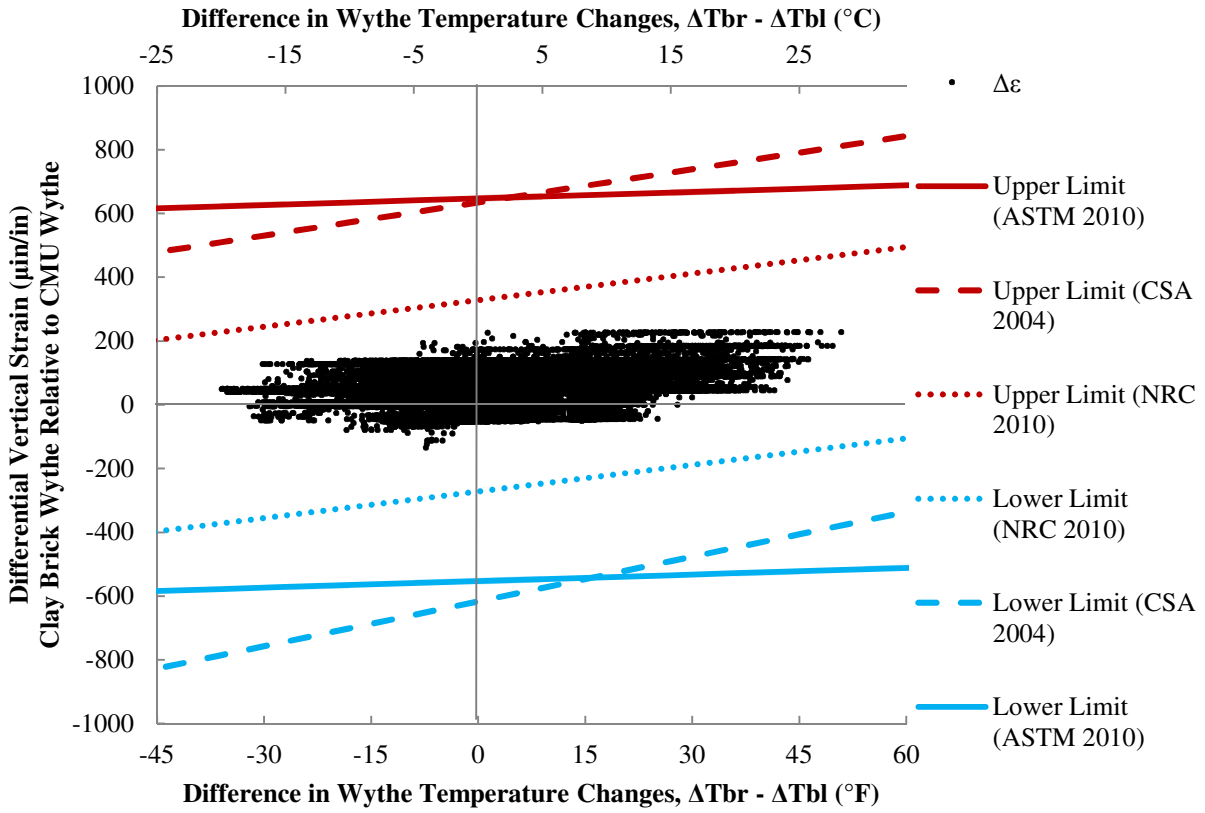

Figure 4 - Comparison of Measured Differential Movements from All Four Walls with Design Limits

When calculating thermal strains to size movement joints, it is important to have an accurate estimate of the facade's mean body temperature in the most extreme environmental conditions expected for the building. Underestimating peak temperature could lead to undersized joints and potentially overstressed masonry veneer.

Overestimating peak temperature could lead to overuse of movement joints, with potentially adverse effects on the aesthetics, moisture management, and costs of masonry cavity walls. As shown in Table 8, the south wall of the St. Albert clock tower regularly experienced a significant amount of solar heating. The hottest temperature recorded was nearly 113 °F (45 °C) on the inner surface of the clay brick veneer of the south wall on September 5, 2013. Though it was late in the year to be experiencing peak temperatures, the outdoor air temperatures at the tower were well above the seasonal norms on September 4 – 5, 2013, reaching as high as 80 °F (27 °C) in the late afternoon. For comparison, a thermal simulation was carried out using WUFI Plus (FIBP (2011)) using an approximate model of the tower and climate data representing a typical meteorological year for Edmonton, Alberta. Taking the veneer temperature to be the average of its inner and outer surface temperatures, the simulation predicted a peak temperature of 120 °F (49 °C) in a typical year. A similar analysis was also performed substituting the recorded indoor and outdoor temperature data collected for boundary conditions instead of the weather data in WUFI's database. The clay brick veneer's peak temperature was estimated to be 129 °F (54 °C) based on that analysis. However, the design temperature of the clay brick veneer of the St. Albert clock tower is 100 to 109 °F (38 to 43 °C) according to the 2010 NBCC Commentaries. As shown in Figure 5, the actual temperature of the clay brick veneer exceeded this design limit by several degrees for three to six hours on September 5, 2013. ASTM C1472-10 on the other hand is more conservative, giving a peak design temperature of 131 to 147 °F (55 to 64 °C). The ASTM design limit was not exceeded at any time.

Looking also at the magnitude of overheating calculated from the 2010 NBCC Commentaries and ASTM C1472-10, it is clear that the 2010 NBCC Commentaries is not conservative. The maximum temperature recorded on the inner surface of the clay brick was 64 °F (35.5 °C) warmer than the outdoor air temperature at the time, far greater than the range of 18 to 27 °F (10 to 15 °C) prescribed in the 2010 NBCC Commentaries and nearly overshooting the range of 49 to 65 °F (27 to 36 °C) calculated from ASTM C1472-10.

Table 8. Measured Facade Temperatures and Comparison with Outdoor Air Temperature

Parameter	North	East	South	West
Maximum facade temperature	87.8 °F (31.0 °C)	103.3 °F (39.6 °C)	112.6 °F (44.8 °C)	109.8 °F (43.2 °C)
Maximum difference between facade and air temperatures	23.2 °F (12.9 °C)	38.5 °F (21.4 °C)	63.9 °F (35.5 °C)	54.2 °F (30.1°C)
Percentage of time where difference exceeds +27 °F (+15 °C)	n/a	0.6%	8.0%	3.4%
Minimum facade temperature	-21.3 °F (-29.6 °C)	-19.5 °F (-28.6 °C)	-20.7 °F (-29.3 °C)	-22.4 °F (-30.2 °C)
Minimum difference between facade and air temperatures	-7.2 °F (-4.0 °C)	-5.6 °F (-3.1 °C)	-4.5 °F (-2.5 °C)	-7.0 °F (-3.9 °C)

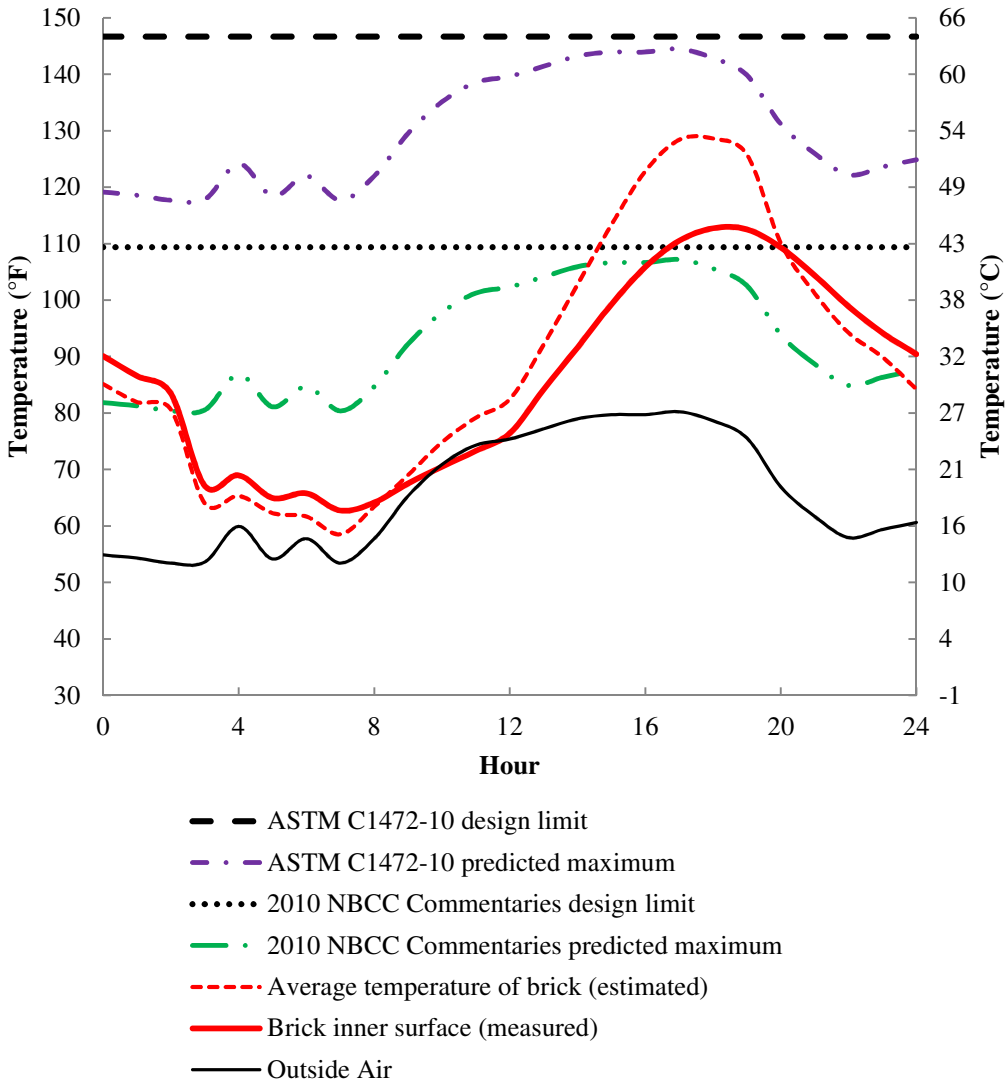

Figure 5 - Temperature of the South Wall on September 5, 2013 Compared with ASTM C1472-10 and 2010 NBCC Commentaries

CONCLUSION

Over a period of 638 days, an hourly record of temperature, humidity, and vertical movements in the masonry cavity walls of a 17-year-old clock tower in St. Albert, Alberta, Canada was obtained and analyzed. The most extreme movements observed were found to be smaller than the peak movements estimated by various design guidelines. However, the observations were in fair agreement with design guidelines regarding the magnitude of reversible movement relative to permanent movement and also the relative contribution of the clay brick wythe to total reversible movement. It was also shown that, while reversible differential movement is strongly correlated with temperature changes in the individual wythes, reversible moisture movements independent of temperature are significant.

Based on the data record so far, some recommendations can be made.

First, the reversible moisture strains given in the 2010 NBCC Commentaries should probably be increased to agree with CSA S304.1-04 and ASTM C1472-10.

Second, the 2010 NBCC Commentaries is not conservative in its estimate of the peak temperature of clay brick veneer. Therefore, the peak design temperature needs to be increased to properly account for solar radiation effects on masonry veneer.

Third, the data supports a coefficient of thermal expansion for fired clay brick masonry consistent with the value prescribed in ASTM C1472-10 or the lower end of the range of values prescribed in Eurocode 6 (CEN (2005)).

Finally, field data from multiple locations covering long time periods is needed in order to calibrate movement joint design guidelines based on an acceptably low probability of exceedance.

ACKNOWLEDGMENTS

Funding was provided by the Natural Sciences and Engineering Research Council of Canada (NSERC) in collaboration with Read Jones Christoffersen. The authors wish to extend their gratitude to the City of St. Albert for granting full access to the clock tower. Finally, the technical assistance of the University of Alberta's technicians Greg Miller and Cameron West are greatly appreciated.

REFERENCES

Amde et al (2007). Amde, A. M., Martin, J.V., Colville, J., "The Effects of Moisture on Compressive Strength and Modulus of Brick Masonry." *TMS Journal,* The Masonry Society, Longmont, CO, Vol. 25 No. 1, pp. 31-40, 2007.

Anand and Gandhi (1983). Anand, S.C., Gandhi, A., "A Finite Element Model to Compute Stresses in Composite Masonry Walls Due to Temperature, Moisture and Creep", *Proceedings of the 3rd Canadian Masonry Symposium,* Edmonton, AB, Canada, June 6-8, 1983 pp. 34.1-34.20, 1983.

ASTM (2010). American Society for Testing and Materials (ASTM), "ASTM C1472-10: Standard Guide for Calculating Movement and Other Effects When Establishing Sealant Joint Width", American Society for Testing and Materials, West Conshohocken, PA, 2010.

BIA (2006). BIA: Brick Industry Association, Technical Note 18: "Volume Changes – Analysis and Effects of Movement", Brick Industry Association, Reston, VA, 2006.

Brooks (1987). Brooks, J.J., "Composite Modelling of Elasticity and Creep of Masonry", Dept. of Civil Engineering Report, University of Leeds, Leeds, United Kingdom, 1987a.

Brooks (1987). Brooks, J.J., "Composite Modelling of Moisture Movement and Thermal Movement of Masonry", Department of Civil Engineering Report, University of Leeds, Leeds, United Kingdom, 1987b.

Brooks and Abdullah (1990). Brooks, J.J., Abdullah, C.S., "Creep and Drying Shrinkage of Concrete Blockwork." *Magazine of Concrete Research,* ICE Virtual Library, pp. 15-22, 1990.

CSA (2004). CSA: Canadian Standards Association CSA S304.1-04, "Design of Masonry Structures" Canadian Standards Association, Mississauga, ON, Canada, 2004.

Davison (1980). Davison, J.I., "Linear Expansion Due to Freezing and Other Properties of Bricks." *Proceedings of the 2nd Canadian Masonry Symposium,* Ottawa, ON, Canada, June 9-11, pp. 13-24, 1980.

Drysdale and Khattab (1995). Drysdale, R., Khattab, M., "Shrinkage Characteristics of Concrete Blocks", *Proceedings of the 7th Canadian Masonry Symposium,* Hamilton, ON, Canada, June 4-7, pp. 950-960, 1995.

CEN (2005). CEN: European Committee for Standardization, *EN 1996-1-1: Eurocode 6: Design of Masonry Structures – Part 1: General – Rules for Reinforced and Unreinforced Masonry,* European Committee for Standardization, Brussels, Belgium, 2005.

Environment Canada (2014). Environment Canada, "Past Weather", 26 April 2014, http://climate.weather.gc.ca/.

Fenton and Suter (1986). Fenton, G.A., Suter, G.T., "Differential Movements and Stresses in High-Rise Masonry Veneers: Analysis", *Canadian Journal of Civil Engineering,* NRC Research Press, Ottawa, ON Canada, pp.700-712, 1986.

Fenton and Suter (1986). Fenton, G.A., Suter, G.T., "Differential Movements and Stresses in High-Rise Masonry Veneers: Case Study," *Canadian Journal of Civil Engineering,* NRC Research Press, Ottawa, ON, Canada, pp. 713-721, 1986.

FERO Corporation (2014). FERO Corporation. "Block Shear™ Connector", www.ferocorp.com/pages/bs_connector/bs_connector.html, December 2014.

FIBP (2011). Fraunhofer Institute for Building Physics, WUFI Plus Version 2.1. Software, Fraunhofer IBP, Stuttgart, Germany, 2011.

Forth et al (2000). Forth, J.P., Brooks, J.J., Tapsir, S.H., "The Effect of Unit Water Absorption on Long-Term Movements of Masonry", *Cement & Concrete Composites,* Elsevier, pp. 273-280, 2000.

Grimm (1975). Grimm, C.T., "Design for Differential Movement in Brick Walls", *Journal of the Structural Division,* ASCE, Reston, VA, pp. 2385-2403, 1975.

Grimm (1982). Grimm, C.T., "Thermal Strain in Brick Masonry", *Proceedings of the 2nd North American Masonry Conference*, College Park, MD, 1982.

Grimm (2000). Grimm, C.T., "Falling Brick Facades", *The Construction Specifier,* Construction Specifications Institute (CSI), Richmond Hill, ON, Canada, pp. 53-56, 2000.

Grimm and Fowler (1979). Grimm, C.T., Fowler, D.W., "Differential Movement in Composite Load-Bearing Masonry Walls", *Journal of the Structural Division,* ASCE, Reston, VA, pp. 1277-1288, 1979.

Hughes and Harvey (1995). Hughes, T.G, Harvey, R.J., "Creep Measured in a Brick Masonry Tower", *Masonry International,* International Masonry Society, Surrey, United Kingdom**,** pp. 50-56, 1995.

ICRI (2008). International Concrete Repair Institute (ICRI), *Guideline No. 410.1-2008: Guide for the Evaluation of Masonry Façade Structures*, International Concrete Repair Institute, Des Plaines, IL, 2008.

Jessop (1980). Jessop, E., "Moisture, Thermal, Elastic, and Creep Properties of Masonry: A State-of-the-Art Report", *Proceedings of the 2nd Canadian Masonry Symposium*, Ottawa, ON, Canada, June 9-11, pp. 505-520, 1980.

Kuzik et al (1999). Kuzik, M., Elwi, A.E., Hatzinikolas, M.A., "Long Term Differential Movements in Masonry Cavity Walls", *Proceedings of the 8th North American Masonry Conference*, Austin, TX, June 6-9, 1999.

Kvande and Lisø (2009). Kvande, T., Lisø, K.R., "Climate Adapted Design of Masonry Structures", *Building and Environment,* Elsevier, pp. 2442-2450, 2009.

Lohonyai et al (2014). Lohonyai, A.J., Korany, Y., Gül, M., "Remote Field Monitoring of Thermal and Moisture Deformations in Masonry Cavity Wall Building Envelopes", *Journal of Performance of Constructed Facilities,* ASCE, Reston, VA, 2014.

MSJC (2011). Masonry Standards Joint Committee. (MSJC), *Building Code Requirements and Specification for Masonry Structures*, The Masonry Society, Longmont, CO, 2011.

NCMA (2005). National Concrete Masonry Association (NCMA), TEK 10-1A: "Crack Control in Concrete Masonry Walls", National Concrete Masonry Association, Herndon, VA, 2005.

NRC (2010). National Research Council of Canada (NRC), *User's Guide – NBC 2010: Structural Commentaries (Part 4 of Division B),* National Research Council of Canada, Ottawa, ON, Canada, 2010.

Peraza (2009). Peraza, D.B., "Special Problems with Composite Multiwythe Masonry Walls", *Proceedings of the 5th Forensic Engineering Congress*, Washington, DC, pp. 66-73, 2009.

Plewes (1970). Plewes, W. G., "Cladding Problems Due to Frame Movements", *Canadian Building Digest 125,* National Research Council of Canada, Ottawa, ON, Canada, 1970.

Plewes (1976). Plewes, W. G., "Vertical Movement of Building Frames and Cladding", *NRCC 15477: Cracks, Movements, and Joints in Buildings,* Ed. C.B. Crawford, National Research Council of Canada, Ottawa, ON, Canada, 1976.

Plewes (1977). Plewes, W. G., "Failure of Brick Facing on High-Rise Buildings", *Canadian Building Digest 185*, National Research Council of Canada, Ottawa, ON, Canada, 1977.

Sayed-Ahmed et al (1998). Sayed-Ahmed, E.Y., Shrive, N.G., Tilleman, D., "Creep Deformation of Clay Masonry Structures: A Parametric Study", *Canadian Journal of Civil Engineering,* NRC Research Press, Ottawa, ON, Canada, pp. 67-80, 1998.

Shrive and England (1981). Shrive, N.G., England, G.L., "Elastic, Creep, and Shrinkage Behaviour of Masonry", *International Journal of Masonry Construction,* United Trade Press Ltd., London, United Kingdom, pp. 103-109, 1981.

Straube and Burnett (2005). Straube, J., Burnett, E., *Building Science for Building Enclosures*, Building Science Press, Westford, MA, 2005.

Suter and Hall (1976). Suter, G.T., Hall, J.S., "How Safe are Our Cladding Connections?" *Proceedings of the 1st Canadian Masonry Symposium*, Calgary, AB, Canada, pp. 95-109, 1976.

Yura (1986). Yura, J.A. "Differential Movement Effects in Steel Shelf Angles", *Journal of Structural Engineering,* ASCE, Reston, VA, pp. 636-652, 1986.

NOTATION

A	=	Solar absorption coefficient
H	=	Heat capacity factor
R^2	=	Coefficient of determination
T_a	=	Design air temperature
$T_{s,max}$	=	Maximum surface temperature
α	=	Coefficient of linear thermal expansion
ΔT	=	Change in temperature
ΔT_{bL}	=	Change in temperature of the concrete block wythe
ΔT_{br}	=	Change in temperature of the clay brick wythe
$\varepsilon_{m,r}$	=	Reversible moisture-related strain
ε_t	=	Thermal strain
ε_{tot}	=	Total reversible strain
ε_{bL}	=	Reversible strain in the concrete block wythe
ε_{br}	=	Reversible strain in the clay brick wythe